New Methods for Computer Tomography Based Ion Thruster Diagnostics and Simulation

IEPC-2024-469

Presented at the 38th International Electric Propulsion Conference, Toulouse, France
June 23-28, 2024

Jörn Krenzer*[1], Felix Reichenbach†[1], and Jochen Schein‡[1]

[1] *Bundeswehr University Munich, Werner-Heisenberg-Weg 39, 85577 Neubiberg, Germany*

Acronyms and Abbreviations

CGLS Conjugate Gradient Least Squares

CT Computed Tomography

EM Expectation-Maximization

ESA European Space Agency

FBP Filtered Back Projection

FDK Feldkamp-Davis-Kress

GSTP General Support Technology Programme

MAR Metal Artifact Reduction

SART Simultaneous Algebraic Reconstruction Technique

SIRT Simultaneous Iterative Reconstruction Technique

µCT Microscopic Computed Tomography Device

I. Introduction

A. Motivation

Non-destructive X-ray imaging of thruster parts and assemblies down to the scale of several micrometers is a key technology for electric propulsion research and engineering. It allows for thorough product assurance, rapid state acquisition and implementation of more detailed simulation models to understand the physics of device wear and erosion.

Being able to inspect parts as 3D density maps allows insight into inner structures hidden from observation. Generating these density maps and also constructing three dimensional mesh objects for further processing depends on the achievable quality of the reconstruction, which is the inverse of Radon's transformation connecting a stack of projections taken from different angles to the original object's structure.

Reconstruction is currently flawed by strong mathematical artifacts induced by the many aligned parts and stark density contrasts commonly found in electric propulsion thrusters.

For the raw image acquisition today's industrial X-ray Microscopic Computed Tomography Devices (µCTs) offer enough performance, but for the step of optimization, mathematical reconstruction and volume generation

*Research Assistant, Institute for Physics, Laboratory for Plasma Technology, joern.krenzer@unibw.de
†Student Assistant, Institute for Physics, Laboratory for Plasma Technology, felix.reichenbach@unibw.de
‡Chairholder, Institute for Physics, Laboratory for Plasma Technology, jochen.schein@unibw.de

no transparent and reviewable software package is currently accessible to the electric propulsion community which is able to tackle the specific properties and requirements of electric thrusters.

This work shows the a comparison of classical and modern reconstruction algorithms which have been investigated to determine the further paths viable to develop transparent reconstruction solutions for usage in electric propulsion diagnostics.

II. Fundamentals

In this section a brief explanation of the functional principle of CT and the reconstruction process will be given. To be concise, mathematical explanations are left out; readers interested in a more thorough theoretical explanation are recommended to refer to literature [1] or, for a brief introduction, the previous work [2] presented at IEPC 2022.

A. X-Ray Tomographic Imaging

As a quick reminder we cover the schematic functional principle of a µCT here. A X-Ray Computed Tomography (CT) device acquires attenuation (dampening) values along rays going from a source through a specimen into a detector array fig. 1. Depending on the setup these radiographs can be one or two dimensional. By rotating the specimen or the device, another radiograph is acquired. The stack of these radiographs is the input for the reconstruction process.

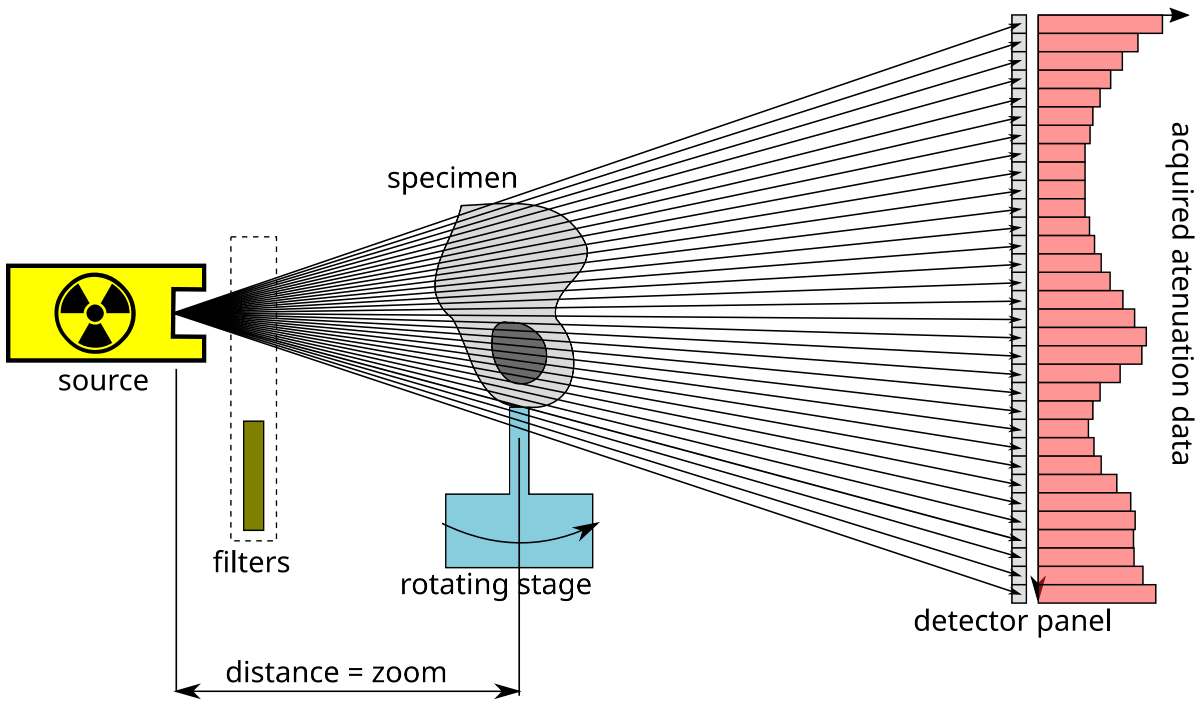

Figure 1: Functioning principle schematic of a simple µCT

CT devices come with different projection geometries, both two and three-dimensional fig. 2. For µCTs, which are best suited for electric propulsion diagnostics the geometry is customary a flat-fan or flat-cone geometry. Flat refers to the detector not being curved towards the source but flat. The projection geometry is crucial information for the reconstruction process and not all algorithms are able to process data acquired in all the possible projection geometries.

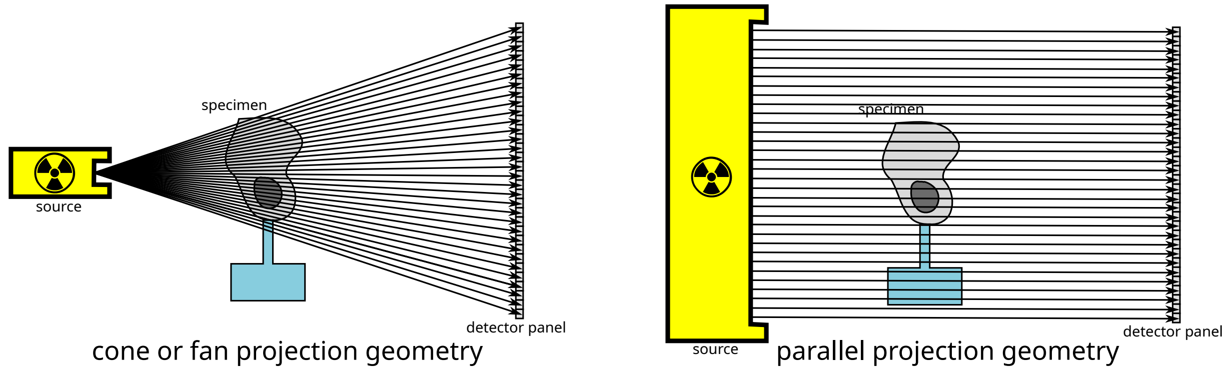

Figure 2: Different projection geometries found typically in CT devices. Both classes of geometries can be realized in a two or three dimensional variants

B. Reconstruction Process

The basis of reconstruction is the implementation of an inverse RADON-tranformation to reverse the integration of attenuation values along each beam-line as seen in fig. 1. One of the oldest algorithms for this is Filtered Back Projection (FBP) to reverse the projection process which works on one projection at a time. Newer algorithms implement iterative approaches, so initial guesses, weights or other techniques to influence reconstruction can be applied in between steps and also simultaneous approaches which take into account data from multiple or all projection layers at once.

As seen in fig. 3 the overall process has several steps of data processing where additional methods can tie in to influence result quality. For iterative algorithms it is possible to directly access each reconstruction step and thus they are well suited for modification.

III. Experimental Approach

The goal of this investigation is the identification of promising reconstruction methods as part of a larger endeavor to develop a specialized workflow for imaging electric propulsion systems in µCTs. For this purpose different reconstruction algorithms are provided with the same input data and results are compared subjectively. As base for the comparison, an earlier reconstruction image using the CT device's included algorithm is to visualize overall improvement against proprietary software which tailored to the device.

A. Selection of Algorithms

The algorithms are chosen for their relevance in practical use and for their perceived better coping capabilities with metal artifacts. Some classical algorithms are chosen as they might be susceptible to artifacts but are in wide-spread use in software included with devices typically well suited for electric propulsion diagnosis. Investigated algorithms are:

- FBP [1]
  - A two dimensional algorithm with high popularity in micro CT device software
  - Low computational cost
  - Said to be prone to strong artifact generation
  - Quality dependent on the filter which is used
- Feldkamp-Davis-Kress (FDK) [3]
  - A three dimensional algorithm with high popularity in micro CT device software
  - Low computational cost
  - Said to be prone to strong artifact generation
- Simultaneous Iterative Reconstruction Technique (SIRT) [4]
  - Available as two and three dimensional variant
  - Iterative algorithm, suitable for iterative artifact reduction techniques

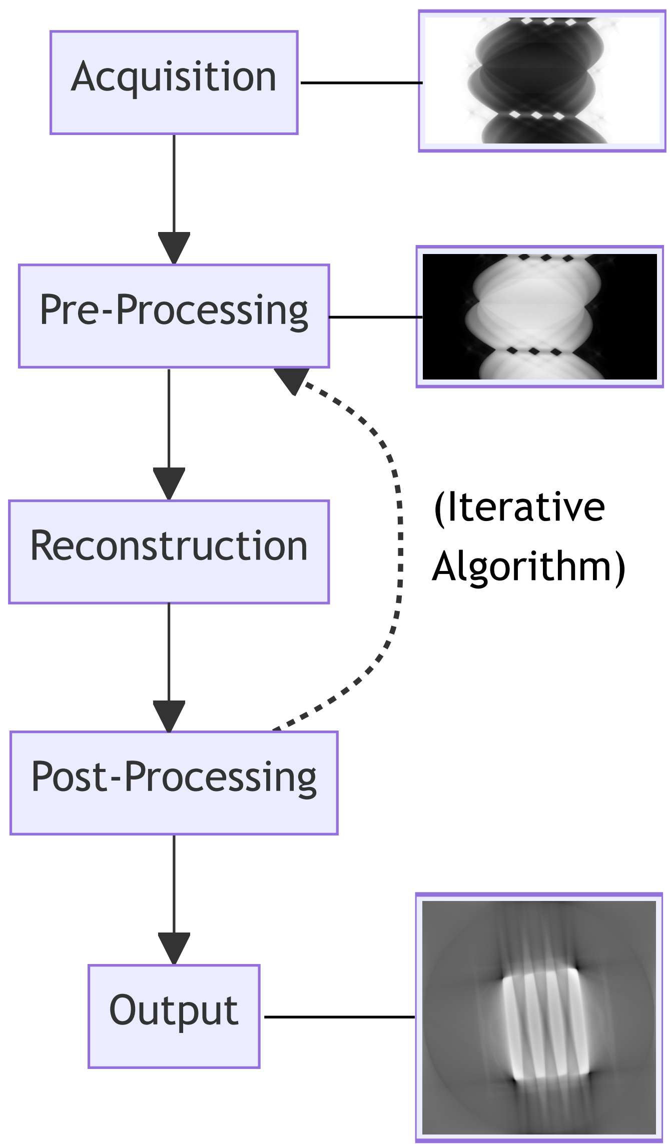

Figure 3: Flow of the reconstruction process. Radiograph data is acquired or loaded, preprocessing yields sinograph. Reconstruction can be iterative in some algorithms allowing for enhanced processing. Postprocessing generates Image stacks for 3 dimensional density data.

    - Medium to high computational cost
    - Generates smooth pictures at the cost of global optimization
    - Better perceived performance with artifacts then FBP and FDK
- Simultaneous Algebraic Reconstruction Technique (SART) [4]
    - Available as two and three dimensional variant
    - Iterative algorithm, suitable for iterative artifact reduction techniques
    - Medium computational cost
    - Generates somewhat noisy pictures but has local optimization
    - Better perceived performance with artifacts then FBP and FDK
- Conjugate Gradient Least Squares (CGLS) [1]
    - Available as two and three dimensional variant
    - Classical, wide-spread algorithm
    - Low to medium computational cost
    - Better perceived performance with artifacts then FBP and FDK
- Expectation-Maximization (EM) [5]
    - A two dimensional, statistical algorithm
    - High computational cost
    - Said to be robust against artifacts at the cost of being highly depended on a good a priori guess of specimen geometry

B. Test Specification

Each algorithm receives the same input data of a phantom which was build to emphasize the structural challenges for CT imaging in a gridded ion thrusters ion optic. See [2] for information on the phantom. Input data was, as is customary in many micro CT systems, acquired in a cone-beam projection geometry.

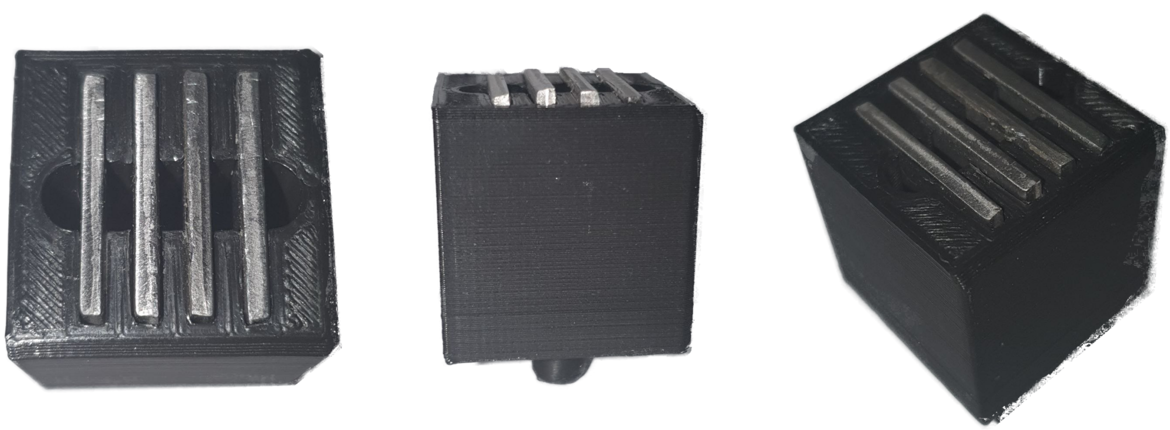

Figure 4: Photographs of the phantom used. The structure with four stainless steel plates in parallel isolated and embedded in plastic models the simplified structure of an electric propulsion ion optic

The phantom, by the close proximity of the parallel metal plates, strongly evokes the metal streaking artifacts and information loss observed in CT survey of gridded ion optics. Thus, any improvement achieved on imaging of the phantom is likely to hold up to the same degree in observation of real world ion optic grids.

Testing of the algorithms is conducted by a dedicated software package written in python 3 to facilitate comparable input and output processes and thereby minimize the influence of data loading and saving operations on the perceived results.

To ensure a comparable implementation-quality of the algorithms, the ASTRA Toolbox was chosen as reconstruction backend [6,7]. A comparison with additional algorithms and alternative implementations was planned using the TomoPy [8] and SVMBIR [9] frameworks, but could not be performed in scope of this work due to the additional integration effort imposed colliding with time constraints.

IV. Discussion

A. Reconstruction Results

In fig. 6 the output of all tested algorithms and a reference picture reconstructed with the µCT device-software (undisclosed algorithm) are presented for comparison.

It should be duly noted, that the pictures are reduced in size and especially dynamic range as 32 bit floating point values cannot be rendered in printing or on normal computer screens without down-sampling the data. These circumstances lead to data-loss cropped to the original data.

Aside from these necessary transformation not further optimizations, e.g. beam-hardening-correction, rotation-artifact-reduction etc. have been applied to assert no interference with achieved quality of reconstruction.

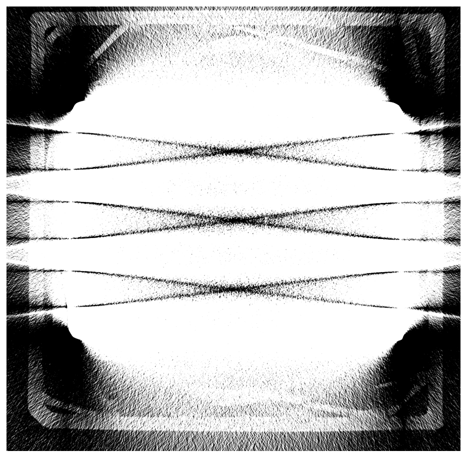

Figure 5: Best reconstruction achieved with device's included software

B. Comparison

It is apparent from fig. 6, that the undisclosed algorithm (fig. 5) in the manufacturer's software is, in our case, performing worst even though it is tailored to the specific device. Thus, it was decided to run also a FBP reconstruction, as this algorithm is very popular especially in more seasoned device software and might be the base of the undisclosed algorithm. This way, it was hoped, the comparison would be more objective and yield better insight in the potential of the algorithms. The performance of FBP depends on the ability of the filter which is used and it turns out, the default filter used by the ASTRA Toolbox is well suited to the tested geometry.

It has to be noted, that almost all modern algorithms (means excluding FBP, FDK and CGLS) are able to receive a priori information and/or weight maps which can greatly help to reduce artifact generation and speed up reconstruction. There were no such information provided in this test, as the establishment of a reliable weighting or first-guess generator is not trivial and must be tailored to the specific class of use-cases.

Further comparison yields, that SART (fig. 6e) generates noisy pictures and thus is deemed less favorable for the typical geometry of electric propulsion ion optics. SIRT generates promising results quite fast even without a priori information, but without this additional data it performs comparable to the classic FBP (given a good filter), FDK and CGLS algorithms. EM is very interesting as it produces high structural contrast, but without a priori data or other methods to reduce the artifacts generate by metal, the streaking severely impacts the usability of the algorithm.

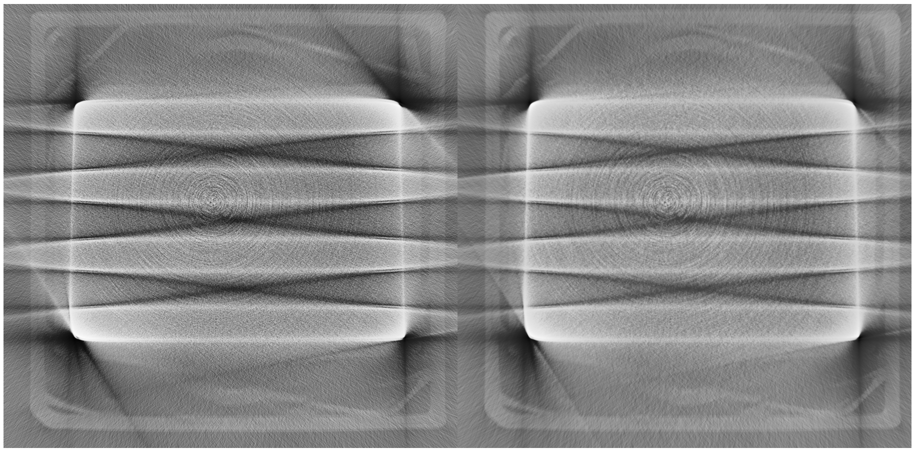

(a) FBP (b) CGLS

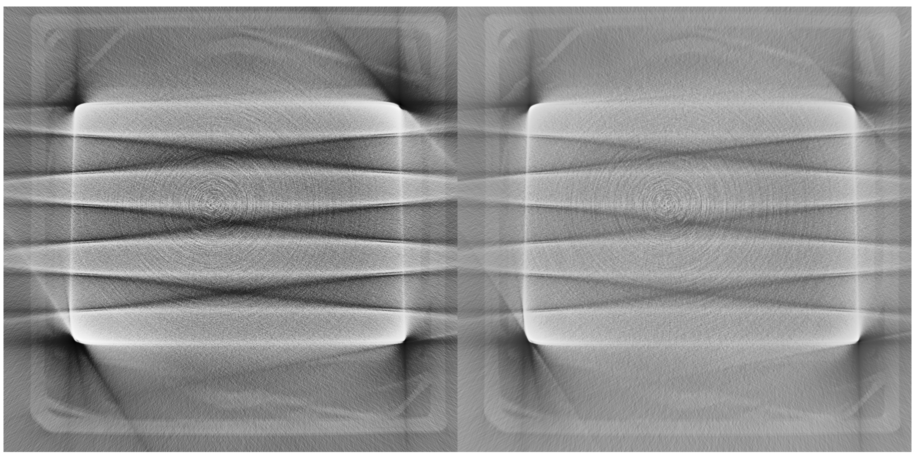

(c) FDK 3-dimensional (d) SIRT

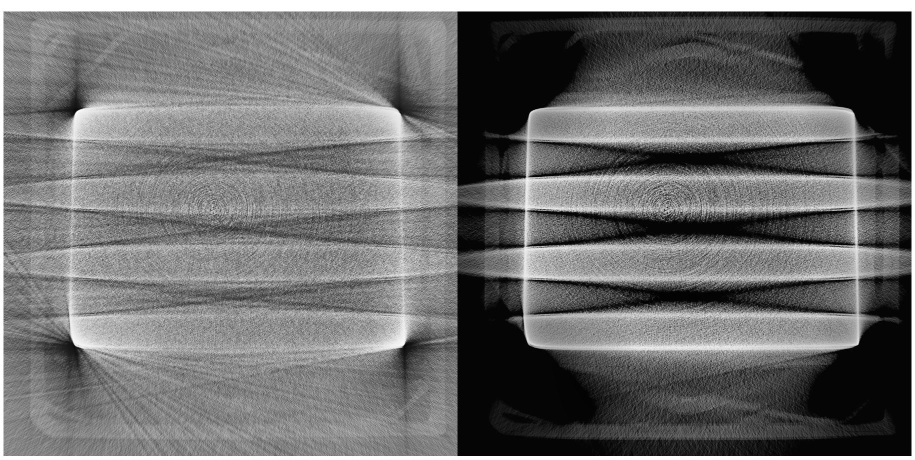

(e) SART (f) EM

Figure 6: These are the post-processed results of the different testes algorithms. Pictures have been adaptively normalized and range-reduced to give a comparable viewing impression in this document.

V. Conclusion

The first conclusion of this endeavor is, that it can be very worthwhile for experimenters to implement their own reconstruction solution instead of using the manufacturer supplied software. The difference in quality, depending on the implementation in the closed source software, can be significant.

Secondly, while modern, especially iterative algorithms perform much better in medical settings, the improvement is much smaller in the setting of electric propulsion ion optics. The implementation of a classic Metal Artifact Reduction (MAR) algorithms [10] was undertaken but did not yield any usable results yet which could be presented here. At the time of writing it is unclear, if this approach is feasible at all with electric propulsion specimen. Further MAR techniques have yet to be investigated for applicability.

It can be assumed, that performance of reconstruction in modern algorithms can be enhanced by introducing a priori data suited to this use-case. Currently the SIRT and EM algorithms are deemed the most favorable candidates for such an approach. Furthermore the implementation of specific metal artifact reduction algorithms adapted to electric propulsion diagnostics seems a viable endeavor.

Acknowledgments

Part of this work was kindly sponsored by the General Support Technology Programme (GSTP) of the European Space Agency (ESA) [11]. Please refer to the references section for details.

References

[1] Herman, G. T., "Fundamentals of Computerized Tomography," Springer, London, 2009. https://doi.org/10.1007/978-1-84628-723-7

[2] Krenzer, J., Reichenbach, F., and Schein, J., "IEPC-2022-260: CT-Imaging in Electrostatic Thruster Ion-Optics," Vols. IEPC-2022, Cambridge, USA, 2022. https://doi.org/10.48550/arXiv.2412.03426

[3] Feldkamp, L. A., Davis, L. C., and Kress, J. W., "Practical Cone-Beam Algorithm," *JOSA A*, Vol. 1, No. 6, 1984, pp. 612–619. https://doi.org/10.1364/JOSAA.1.000612

[4] Andersen, A. H., and Kak, A. C., "Simultaneous Algebraic Reconstruction Technique (SART): A Superior Implementation of the ART Algorithm," *Ultrasonic Imaging*, Vol. 6, No. 1, 1984, pp. 81–94. https://doi.org/10.1016/0161-7346(84)90008-7

[5] Lange, K., and Carson, R., "EM reconstruction algorithms for emission and transmission tomography," *Journal of Computer Assisted Tomography*, Vol. 8, No. 2, 1984, pp. 306–316.

[6] van Aarle, W., Palenstijn, W. J., De Beenhouwer, J., Altantzis, T., Bals, S., Batenburg, K. J., and Sijbers, J., "The ASTRA Toolbox: A Platform for Advanced Algorithm Development in Electron Tomography," *Ultramicroscopy*, Vol. 157, 2015, pp. 35–47. https://doi.org/10.1016/j.ultramic.2015.05.002

[7] Aarle, W. van, Palenstijn, W. J., Cant, J., Janssens, E., Bleichrodt, F., Dabravolski, A., Beenhouwer, J. D., Batenburg, K. J., and Sijbers, J., "Fast and Flexible X-Ray Tomography Using the ASTRA Toolbox," *Optics Express*, Vol. 24, No. 22, 2016, pp. 25129–25147. https://doi.org/10.1364/OE.24.025129

[8] Gürsoy, D., De Carlo, F., Xiao, X., and Jacobsen, C., "TomoPy: A Framework for the Analysis of Synchrotron Tomographic Data," *Journal of Synchrotron Radiation*, Vol. 21, No. 5, 2014, pp. 1188–1193. https://doi.org/10.1107/S1600577514013939

[9] Team, S. D., "Super-Voxel Model Based Iterative Reconstruction (SVMBIR)," 2024.

[10] Chang, Y.-B., Xu, D., and Zamyatin, A. A., "Metal Artifact Reduction Algorithm for Single Energy and Dual Energy CT Scans," Anaheim, CA, USA, 2012. https://doi.org/10.1109/NSSMIC.2012.6551781

[11] ESA, Ed., "4000124912/18/NL/KML – Improvement Of The Lifetime Of Electric Propulsion Thrusters Using Different Propellant By Reducing Sputtering Effects On Materials," 2018.